

1 **Convergent evolution of seasonal camouflage in response to reduced snow cover across the**  
2 **snowshoe hare range**

3 Matthew R. Jones<sup>1,2</sup>, L. Scott Mills<sup>3,4</sup>, Jeffrey D. Jensen<sup>2</sup>, Jeffrey M. Good<sup>1,3</sup>

4 <sup>1</sup>Division of Biological Sciences, University of Montana, Missoula, MT 59812, USA.

5 <sup>2</sup>School of Life Sciences, Arizona State University, Tempe, AZ 85281, USA

6 <sup>3</sup>Wildlife Biology Program, University of Montana, Missoula, MT 59812, USA.

7 <sup>4</sup>Office of Research and Creative Scholarship, University of Montana, Missoula, MT 59812,  
8 USA.

9 Corresponding authors: jeffrey.good@umontana.edu, matthew.r.jones.1@asu.edu

10 Key words: climate change, dominance, local adaptation, migration, parallel evolution

11 **Abstract**

12 Determining how different populations adapt to similar environments is fundamental to  
13 understanding the limits of adaptation under rapidly changing environments. Snowshoe hares  
14 (*Lepus americanus*) molt into white winter coats to remain camouflaged in snowy environments.  
15 In warmer climates across a small portion of their range hares have evolved brown winter  
16 camouflage – an adaptation that may spread under climate change. We used extensive genotype,  
17 exome, and whole genome data to 1) resolve range-wide patterns of population structure and  
18 gene flow in snowshoe hares and 2) investigate the factors shaping the origins and distribution of  
19 winter-brown camouflage variation across the range. In coastal Pacific Northwest (PNW)  
20 populations, winter-brown camouflage is known to be determined by a single recessive  
21 haplotype at the *Agouti* pigmentation gene. Our phylogeographic analyses revealed deep  
22 historical structure and limited gene flow between PNW and more northern Boreal populations,  
23 where winter-brown camouflage is rare but widespread along the range edge. We sequenced the  
24 genome of a winter-brown Alaskan hare and show that it does not possess the winter-brown  
25 PNW *Agouti* haplotype, and thus represents a convergent phenotype that arose through  
26 independent mutations. However, the winter-brown PNW haplotype is present at low frequency  
27 in a distant winter-white population from Montana, consistent with a model in which strongly  
28 deleterious recessive variants spread easily across space because they are masked from selection  
29 at low frequency. Simulations show that if annual snow cover were to dramatically reduce,  
30 positive selection would likely drive the *Agouti* allele to eventual fixation in Montana, although  
31 the initial increase in allele frequency would be extremely slow due to the same masking effect.  
32 Our findings underscore how allelic dominance can shape the geographic extent and rate of  
33 convergent adaptation in response to rapidly changing environments.

## 34 **Introduction**

35           In response to a shared selection pressure, populations may adapt through the migration  
36 of beneficial alleles or through independent mutations that result in the evolution of convergent  
37 phenotypes (Haldane, 1932; Ralph & Coop, 2015; Wright, 1931). Distinguishing between these  
38 scenarios is crucial to understand the capacity of populations to adapt rapidly to environmental  
39 change (Bridle & Vines, 2007; Hoffmann & Sgrò, 2011; Ralph & Coop, 2015). If gene flow  
40 between populations is sufficiently high, then beneficial variation may spread quickly (Fisher,  
41 1937) and potentially allow for rapid adaptive responses to changing environments (Bay et al.,  
42 2017). However, the spread of adaptive variation may be limited at broad geographic scales, and  
43 populations may have to rely on independent standing genetic variation or new mutations to  
44 evolve convergent traits. While there is considerable evidence for both adaptation through gene  
45 flow and independent mutations in nature (Dobler, Dalla, Wagschal, & Agrawal, 2012; Hoekstra,  
46 Krenz, & Nachman, 2005; Hoekstra & Nachman, 2003; Kreiner et al., 2019; Marques et al.,  
47 2017; Rosenblum, Römpler, Schöneberg, & Hoekstra, 2010; Steiner, Rompler, Boettger,  
48 Schoneberg, & Hoekstra, 2008), few empirical studies have examined the specific factors that  
49 influence these outcomes in natural populations (Ralph & Coop, 2015).

50           When a species range encompasses a mosaic of habitats, the relative probability of  
51 adaptation through gene flow versus independent mutation is predicted to be primarily a function  
52 of the distance between habitat patches (in units of dispersal distance) and the strength of  
53 selection against locally adaptive alleles in intervening habitats (Ralph & Coop, 2010, 2015;  
54 Slatkin, 1973). In general, as distance between patches and the strength of purifying selection in  
55 intervening habitats increases, so does the relative probability of adaptation through independent  
56 mutations. Adaptation via independent mutations is therefore predicted to be more common in

57 widespread populations where dispersal distance is short relative to the total range size (Ralph &  
58 Coop, 2010). For example, rock pocket mice (*Chaetodipus intermedius*) have repeatedly evolved  
59 melanistic coats across patchy lava flows in the southwestern United States. Although substantial  
60 gene flow between adjacent lava flows has likely resulted in the migration of melanic alleles  
61 (Hoekstra et al., 2005), melanism is attributed to different mutations across disparate lava flows  
62 (Harris et al., 2019; Hoekstra & Nachman, 2003; Nachman, Hoekstra, & D'Agostino, 2003a).  
63 Theoretical models further predict that the relative probability of adaptation via independent  
64 mutations increases rapidly with distance between lava flows (over the scale of tens to hundreds  
65 of kilometers; Ralph and Coop 2015), due in large part to strong selection against coat color  
66 mismatch (Barrett et al., 2019; Hoekstra, Drumm, & Nachman, 2004; Pfeifer et al., 2018). Thus,  
67 there is a clear tradeoff between dispersal distance and the strength of purifying selection  
68 strength that strongly dictates the probability of adaptation through convergent evolution or gene  
69 flow.

70         The effect of genetic dominance on the probability of convergent evolution has not yet  
71 been thoroughly explored (Ralph & Coop, 2015). ‘Haldane’s sieve’ (Turner, 1981) predicts that  
72 *de novo* dominant mutations enjoy a much greater probability of fixation compared to *de novo*  
73 recessive mutations (probability of fixation  $\approx 2hs$ ), because rare dominant mutations are visible to  
74 selection (Haldane, 1924). As *de novo* beneficial recessives are masked to selection when rare,  
75 those that do ultimately reach fixation may spend a longer period of time drifting at low  
76 frequency (Teshima & Przeworski, 2006). Likewise, rare recessive migrant alleles are expected  
77 to exhibit the same behavior, which may allow more time for mutation to generate ‘competing’  
78 convergent phenotypes upon which selection can act. However, Orr and Betancourt (2001)  
79 demonstrated that genetic dominance has no effect on the probability of fixation for alleles in

80 mutation-selection balance because recessive alleles have a higher mutation-selection balance  
81 frequency. Thus, for relatively high amounts of gene flow, genetic dominance may have little to  
82 no effect on the probability of adaptation via migration versus *de novo* mutation. In fact, the  
83 masking of low frequency recessive alleles may result in weaker purifying selection in  
84 intervening habitats therefore facilitating the spread of adaptive variation through gene flow  
85 (Ralph & Coop, 2015), although this hypothesis remains to be tested.

86         Snowshoe hares (*Lepus americanus*) are one of at least 21 species that have evolved  
87 seasonal molts to white winter coats to maintain camouflage in snowy winter environments.  
88 Because color molts are cued by photoperiod, and hence may become mismatched under rapidly  
89 changing environments (Mills et al., 2013; Zimova et al., 2018), seasonal camouflage provides a  
90 useful trait to understand adaptation to climate change (Jones et al., 2018; Mills et al., 2018,  
91 2013; Zimova et al., 2018; Zimova, Mills, & Nowak, 2016). Reduction in the extent and duration  
92 of snow cover is one of the strongest signatures of climate change in the Northern hemisphere  
93 (Brown & Mote, 2009; Knowles et al., 2006), suggesting that selection should increasingly favor  
94 delayed winter-white molts in snowshoe hares to reduce the total duration of coat color  
95 mismatch. However, seasonal color molts develop relatively slowly in most seasonally changing  
96 species (e.g., 40 days in hares, Mills et al. 2013) and appear to require some minimum duration  
97 of annual snow cover to be beneficial. Below a species-specific threshold, populations are  
98 predicted to maintain brown coloration during the winter (Mills et al., 2018). Consistent with  
99 this, snowshoe hares maintain brown winter camouflage in some temperate environments with  
100 reduced snow cover (Nagorsen, 1983), a strategy that should be increasingly favored under  
101 climate change (Jones et al., 2018; Mills et al., 2018).

102 Winter-brown snowshoe hares are common in coastal regions of the Pacific Northwest  
103 (PNW), where this Mendelian trait is determined by a recessive variant of the *Agouti*  
104 pigmentation gene (Jones et al. 2018). The locally adaptive *Agouti* variant was introduced into  
105 snowshoe hares by introgression with black-tailed jackrabbits ~9-18 thousand years ago (kya)  
106 and subsequently experienced a local selective sweep within the last few thousand years (Jones  
107 et al. 2019). Occasional records of winter-brown camouflage also occur north of the PNW along  
108 the Pacific coast of Canada and southern Alaska, and in some eastern North American  
109 populations (Gigliotti et al. 2017; Mills et al. 2018). Although hares are expected to be more or  
110 less continuously distributed along suitable coastal environments of western North America,  
111 there is a deep genetic split between northern populations of ‘Boreal’ hares and populations from  
112 the PNW and southern Rocky Mountains with little evidence of recent gene flow (Cheng,  
113 Hodges, Melo-Ferreira, Alves, & Mills, 2014; Melo-Ferreira, Seixas, Cheng, Mills, & Alves,  
114 2014). Given this historic population structure, it remains unclear whether the distribution of  
115 winter-brown camouflage across populations from disparate parts of the range reflects  
116 independent genetic origins (i.e. trait convergence) or spread of the introgressed PNW *Agouti*  
117 allele.

118 Here, we use new and previously published genetic data to investigate the roles of gene  
119 flow and mutation in shaping the evolution of winter-brown camouflage across populations of  
120 snowshoe hares. We first combined previously published microsatellite ( $n=853$  individuals, 8  
121 loci) with new and published whole exome data ( $n=95$  individuals) to resolve range-wide  
122 patterns of population history and gene flow in snowshoe hares, which provides crucial context  
123 for understanding the historical spread and adaptive potential for winter-brown camouflage to  
124 climate change. We then generated whole genome sequence (WGS) data of a winter-brown

125 Alaska (AK) hare to test whether winter-brown camouflage in Boreal snowshoe hares arose  
126 independently from PNW populations, located ~3000 km away. Next, to understand the  
127 geographic limits of the recessive PNW *Agouti* allele, we used pooled WGS data to estimate its  
128 frequency in a winter-white population from Montana (MT), approximately 600 km in a straight-  
129 line from the closest winter-brown PNW population. Finally, we used both theoretical  
130 predictions and simulations to understand the factors influencing the geographic scope of the  
131 PNW *Agouti* allele and its potential to contribute to rapid adaptation in response to warming  
132 climates.

133

## 134 **Methods**

### 135 Samples and genomic data generation

136 To resolve patterns of range-wide population structure, we performed targeted whole exome  
137 enrichment of 12 snowshoe hares previously sampled from 12 localities across Canada, Alaska,  
138 and the eastern United States and three hares from the southern Rocky Mountains (representing  
139 the Boreal and Rockies lineages as defined by Cheng et al. (2014)). The targeted whole exome  
140 capture was designed by Jones et al. (2018) to enrich for ~99% of genic regions annotated in the  
141 European rabbit (*Oryctolagus cuniculus*) genome (61.7-Mb spanning 213,164 intervals; ~25-Mb  
142 protein-coding exons, ~28-Mb untranslated region, ~9-Mb intronic or intergenic). We followed  
143 the library preparation protocols outlined in Jones et al. (2018) and sequenced libraries on one  
144 lane of Illumina HiSeq2500 with paired-end 100 bp reads (HudsonAlpha Institute for  
145 Biotechnology; Huntsville, AL). Exome sequences for Boreal and Rockies snowshoe hares were  
146 combined with published whole exome data (Jones et al. 2018) from 80 PNW snowshoe hares  
147 ( $n=95$  total, Table S1), including a monomorphic winter-brown population from southeast

148 British Columbia (BC1,  $n=14$ ), a monomorphic winter-white population from Seeley Lake area  
149 in western MT ( $n=14$ ), and two polymorphic coat color populations from Oregon (OR,  $n=26$ ;  
150 two localities) and Washington (WA,  $n=26$ ; Jones et al. 2018).

151 To resolve the historical spread of the winter-brown PNW *Agouti* allele, we performed  
152 whole genome sequencing of a winter-brown snowshoe hare museum specimen (AK) from  
153 southwest Alaska first noted by Link Olson and later obtained through loan from University of  
154 Alaska Museum of the North (UAM 116170, collected on 4 January 2013). We also performed  
155 whole genome sequencing on a DNA pool of 81 snowshoe hares from two localities in Glacier  
156 National Park, MT (Table S1). We extracted genomic DNA from muscle tissue of the AK hare  
157 sample following the Qiagen DNeasy Blood and Tissue kit protocol (Qiagen, Valencia, CA). For  
158 the pooled MT whole genome sequencing, we pooled previously extracted DNA samples (Cheng  
159 et al., 2014) in approximately equimolar quantities based on Qubit concentrations (Invitrogen  
160 Qubit Quantitation system LTI). We then prepared genomic libraries for all samples following  
161 the KAPA Hyper prep kit manufacturer's protocol. We sheared genomic DNA to ~300 bp using  
162 a Covaris E220evolution ultrasonicator and performed a stringent size selection using a custom-  
163 prepared carboxyl-coated magnetic bead mix (Rohland & Reich, 2012). We determined indexing  
164 PCR cycle number for each library with quantitative PCR (qPCR) on a Stratagene Mx3000P  
165 thermocycler (Applied Biosystems) using a DyNAmo Flash SYBR Green qPCR kit (Thermo  
166 Fisher Scientific). Final libraries were size-selected again with carboxyl-coated magnetic beads,  
167 quantified with a Qubit (Thermo Fisher Scientific), and pooled for sequencing by Novogene  
168 (Novogene Corporation Ltd.; Davis, CA) on two lanes of Illumina HiSeq4000 using paired-end  
169 150bp reads. The whole genome sequence from the AK hare was combined with previously  
170 published whole genome sequencing of five black-tailed jackrabbits, three winter-brown

171 snowshoe hares from OR, WA, and BC1, and three winter white snowshoe hares from MT, a  
172 hare from Utah (UT), and a hare from Pennsylvania (PA; Jones et al. 2018, Table S1).

173

#### 174 Read processing and variant calling

175 For all raw Illumina sequence data, we trimmed adapters and low-quality bases (mean phred-  
176 scaled quality score <15 across 4 bp window) using Trimmomatic v0.35 (Bolger, Lohse, &  
177 Usadel, 2014) and merged paired-end reads overlapping more than 10 bp and with lower than  
178 10% mismatched bases using FLASH2 (Magoč & Salzberg, 2011).

179       Whole genome sequence data were mapped to either a snowshoe hare or black-tailed  
180 jackrabbit pseudoreference (see Jones et al. 2018 for details) using default settings in BWA-  
181 MEM v0.7.12 (Li, 2013). We used *PicardTools* to remove duplicate reads with the  
182 MarkDuplicates function and assigned read group information with the  
183 AddOrReplaceReadGroups function. Using GATK v3.4.046 (McKenna et al., 2010), we then  
184 identified poorly aligned genomic regions with RealignerTargetCreator and locally realigned  
185 sequence data in these regions with IndelRealigner. We performed population-level multi-sample  
186 variant calling using default settings with the GATK UnifiedGenotyper. Here, we called variants  
187 separately for each previously defined snowshoe hare population genetic cluster (i.e., Boreal,  
188 Rockies, BC1, MT, OR, and WA) and for black-tailed jackrabbits. We performed variant  
189 filtration in VCFtools v0.1.14 (Danecek et al., 2011). For whole exome and whole genome data,  
190 we filtered genotypes with individual coverage <5× or >70× or with a phred-scaled quality score  
191 <30. Additionally, we removed all indel variants and filtered SNPs with a phred-scaled quality  
192 score <30, Hardy-Weinberg  $P < 0.001$ . We required that sites have no missing data across  
193 individuals.

194

195 Range-wide population genetic structure and gene flow

196 We inferred a maximum likelihood tree with a general time reversible model in RAxML v8.2.8  
197 (Stamatakis, 2014) using a subset of the concatenated snowshoe hare exome data ( $n=12$  Boreal  
198 hares,  $n=3$  Rockies hares,  $n=12$  PNW hares; 21,167,932 total sites) with European rabbit  
199 (*Oryctolagus cuniculus*) as the outgroup. Using this maximum likelihood tree as a starting tree,  
200 we estimated a maximum clade credibility tree and node ages with a constant population size  
201 coalescent model in BEAST 2 (Bouckaert et al., 2014). We assumed a strict molecular clock and  
202 an HKY substitution model using empirical base frequencies. We specified default priors for the  
203 kappa parameter, gamma shape parameter, and population size parameter and used a gamma  
204 distribution ( $\alpha=0.0344$ ,  $\beta=1$ ) as a prior for the clock rate parameter. We ran the MCMC  
205 for 5 million steps and calibrated divergence times using a log-normal distribution for the  
206 *Oryctolagus-Lepus* node age with a median of 11.8 million years (95% prior density: 9.8–14.3;  
207 Matthee et al. 2004). We also performed a species-tree analysis using gene trees in ASTRAL  
208 v5.6.3 (Zhang, Rabiee, Sayyari, & Mirarab, 2018). Gene trees were generated across 200 kb  
209 windows (excluding windows with fewer than 500 sequenced bases) using RAxML with a  
210 GTR+gamma model and rapid bootstrap analysis (-f a -# 10). We collapse nodes on gene trees  
211 with low bootstrap support values ( $\leq 10$ ) and performed ASTRAL analyses on the collapsed  
212 gene trees using default settings.

213 To test for signatures of population structure and gene flow among lineages, we  
214 performed a population cluster analysis in ADMIXTURE v1.3.0 (Alexander, Novembre, & Lange,  
215 2009). We tested  $K$  values from 1-10 (representing the number of population clusters) and  
216 selected the  $K$  value with the lowest cross-validation error. We also estimated range-wide

217 effective migration and diversity surfaces with EEMS (Petkova, Novembre, & Stephens, 2016)  
218 using extensive microsatellite data ( $n=853$  individuals, 8 loci) generated by Cheng et al. (2014).  
219 Varying the number of demes (50, 100, and 200) had little effect on estimates of effective rates  
220 of migration and diversity, therefore we only report results for 200 demes. We used default  
221 hyper-parameter values and tuned the proposal variances such that proposals were accepted  
222 approximately 30% of the time. We ran EEMS for 2 million iterations with a burn-in of 1 million  
223 iterations and thinning iteration of 9999. Runs produced strong correlations between observed  
224 and expected genetic dissimilarity both within and between demes, indicating good model fit.

225

#### 226 Geographic distribution of the PNW *Agouti* allele

227 The winter-brown AK snowshoe hare was collected approximately 3000 km (via the Pacific  
228 coast) from Vancouver, BC, the northern limit of winter-brown PNW hare populations (Jones et  
229 al., 2018). To test whether the introgressed PNW *Agouti* allele has seeded winter-brown  
230 camouflage in southwest AK, we generated a tree of the PNW *Agouti* haplotype region from our  
231 whole genome sequence data of winter-brown and winter-white snowshoe hares ( $n=7$ ) and black-  
232 tailed jackrabbits ( $n=5$ ). We defined the PNW *Agouti* haplotype region (chr4:5,340,275 –  
233 5,633,020, oryCun2 coordinates) based on the location of the introgressed black-tailed jackrabbit  
234 tract identified by Jones et al. (2018) using a hidden Markov model. We then inferred a  
235 maximum likelihood phylogeny for this interval using RAxML (Stamatakis, 2014) as above.  
236 Node support values were generated from 1000 replicate bootstrap runs.

237 We also estimated the frequency of the PNW *Agouti* haplotype among pooled individuals  
238 from two localities in MT ( $n=81$ ) that are 575 km and 627 km from the polymorphic sampling  
239 locality in WA, where winter-brown camouflage is relatively common. We used PoPoolation2

240 (Kofler et al., 2011) to calculate the frequency of the winter brown-associated alleles at 555 sites  
241 across the introgressed *Agouti* haplotype (chr4: 5,340,275 – 5,633,020). These positions were  
242 previously shown to be strongly associated with coat color based on a likelihood ratio test of  
243 allele frequency differences between winter-brown and winter-white individuals from low  
244 coverage whole genome sequence data (Jones et al. 2018). We summed the counts of winter-  
245 white and winter-brown alleles across all positions to estimate both the mean and standard  
246 deviation of winter-brown allele frequency. We excluded seven positions with unusually high  
247 frequencies of the winter-brown allele (~45-100%) supported by reads that did not otherwise  
248 carry brown-associated alleles (i.e., incongruent haplotype information), as these likely reflect  
249 sequencing errors.

250

#### 251 Probability of convergent adaptation through independent mutation

252 To compare the observed spread of the PNW *Agouti* allele to theoretical expectations, we  
253 estimated the relative probability of adaptation via independent mutations with distance from a  
254 focal habitat patch using the model developed by Ralph and Coop (2015, equation 12) under a  
255 range of conditions. Since the relative probability of adaptation through migration or *de novo*  
256 mutation depends strongly on the rate at which mutations generate convergent phenotypes  
257 (Ralph & Coop, 2015), we tested a range of plausible mutation rates. A previous study using  
258 over 7 million house mice estimated a mean rate of spontaneous visible coat color mutations of  
259  $11e^{-6}$  per locus/gamete (Schlager & Dickie, 1971), which is ~1930× higher than the average  
260 genome-wide germline per site mutation rate ( $5.7e^{-9}$  per site/gamete; Milholland et al. 2017).  
261 Given a genome-wide mutation rate of  $2.35e^{-9}$  per site/generation for rabbits (Carneiro et al.,  
262 2012), we tested a high mutation rate of  $\mu=4.54e^{-6}$  (i.e., the overall expected rate of visible coat

263 color mutations) and a low mutation rate of  $\mu=4.54e^{-8}$  (i.e., assuming only 1% of coat color  
264 mutations would lead to brown winter camouflage). We also tested how strong ( $s_m=0.01$ ),  
265 moderate ( $s_m=0.001$ ), or weak ( $s_m=0.0001$ ) purifying selection against the winter-brown allele in  
266 intervening (i.e., snow-covered) habitats influences the probability of adaptation through  
267 independent mutations. We assumed a relatively high mean dispersal distance of 2 km (Gillis &  
268 Krebs, 1999), which is likely to produce a conservative estimate of the probability of adaptation  
269 via independent mutation. We also assumed that the width of the secondary habitat patch was  
270 relatively small ( $w=1$  or  $\sim 6-45$  km, depending on  $s_m$ ), which is consistent with observations of  
271 winter-brown camouflage at low frequency along portions of the range edge. Finally, we  
272 assumed  $d=1$  (dimension of the habitat),  $C=1$ , and  $\gamma=0.5$ .

273

#### 274 Simulations of selection on migrant alleles with genetic dominance

275 Theory predicts that allelic dominance should not influence a mutation's probability of fixation  
276 under positive selection if it starts in mutation/migration-selection balance (Orr & Betancourt,  
277 2001). Nonetheless, rare recessive mutations may increase in frequency more slowly relative to  
278 rare dominant mutations because they are initially invisible to selection, allowing more  
279 opportunity for competition from convergent phenotypes arising through independent mutations.  
280 We used simulations to test how the genetic dominance of alleles at equivalent mutation-  
281 selection equilibrium frequencies influences the probability and rate of adaptation to new  
282 habitats when environmental conditions change. In SLiM 3.0 (Haller & Messer, 2019) we  
283 performed 100 simulations of the MT population (estimated  $N_e=245430$ ; Jones et al. 2019) with  
284 a positively selected recessive mutation ( $s=0.01$ ,  $h=0$ ) starting at the inferred frequency of the  
285 PNW *Agouti* allele in MT ( $p$ ). We assumed that  $p$  reflects the equilibrium frequency ( $x$ ) between

286 the migration rate of the allele into the environment ( $m$ ) and the selection coefficient against the  
287 allele ( $s$ ), which is given as  $\sqrt{\frac{m}{s}}$  for a recessive mutation. Given that  $x$  for a dominant mutation is  
288 simply  $\frac{m}{s}$ , we calculated  $x$  of an equivalent dominant mutation (same values of  $m$  and  $s$ ) as simple  
289  $p^2$ . We then repeated these simulations for a positively selected ( $s=0.01$ ), completely dominant  
290 allele ( $h=1$ ) starting at its expected mutation-selection balance frequency. For each simulation we  
291 tracked the frequency of the selected allele until it was either fixed or lost. To validate these  
292 simulations, we compared the probabilities of allelic fixation from simulations to fixation  
293 probabilities analytically derived by Kimura (1957). To test for significant differences in fixation  
294 probabilities and rates of adaptation between recessive and dominant mutations we used  
295 Student's t-tests in R (R Core Team, 2018).

296

## 297 **Results**

### 298 Snowshoe hare phylogeography

299 We combined previously generated whole exome data for 80 PNW snowshoe hares (mean  
300 coverage  $21\times \pm 7.6$  per individual) with new whole exomes of 15 hares across the range  
301 sequenced to a mean coverage of  $20.2\times \pm 8.2$  (Fig. 1A). Exome-wide phylogenetic analyses  
302 show three broad phylogeographic groups of snowshoe hares (Fig. 1B) with unambiguous  
303 ASTRAL support scores using 6582 gene trees, consistent with previous studies (Cheng et al.  
304 2014; Melo-Ferreira et al. 2014). However, ~12-25% of SNPs within phylogeographic groups  
305 appear to be shared across some population boundaries (Table 1), indicating some amount of  
306 shared ancestral variation or gene flow. We estimated that snowshoe hares from Canada, Alaska,  
307 and the eastern United States—representing the Boreal lineage—diverged approximately 97.2  
308 kya (95% posterior density: 77.4-120.8 kya) from PNW and Rockies snowshoe hares (Fig. 1B).

309 PNW and Rockies hare populations are estimated to have split approximately 47.1 kya (95%  
310 posterior density: 37.2-58.2 kya).

311 Population structure analyses in ADMIXTURE also found strongest support for three  
312 population clusters, although MT snowshoe hares (in the PNW lineage) showed 11-16% of their  
313 ancestry assigned to the Rockies lineage, indicating ongoing gene flow or continuous genetic  
314 structure (Fig. 1C). The ADMIXTURE analysis also indicated little apparent gene flow between the  
315 Boreal lineage and PNW or Rockies lineages. Likewise, microsatellite-based estimates of  
316 effective migration surfaces revealed that effective migration rates are approximately 100-fold  
317 lower than the range-wide average near the apparent zone of contact between PNW and Boreal  
318 lineages in western North America (Fig. 2A). We also estimated relatively low effective  
319 migration rates across the southwestern edge of snowshoe hare range (western US;  $\log(m) \approx -1$ ,  
320 or 10-fold lower than the mean). In contrast, effective migration rates in the northwest part of the  
321 range (Alaska and western Canada) appeared relatively high (~10-fold higher than the mean).  
322 Effective diversity surfaces show that the highest relative genetic diversity occurs in the eastern  
323 extent (Boreal lineage) and southwestern extent (PNW lineage) of the snowshoe hare range (Fig.  
324 2B), consistent with previous studies suggesting that these regions were likely glacial refugia  
325 (Cheng et al., 2014). Relative genetic diversity gradually decreased moving from east to west  
326 across the Boreal range and the lowest genetic diversity was observed in the Rocky Mountain  
327 lineage, distributed across the western US.

328

### 329 Convergent evolution and the distribution of winter-brown camouflage variation

330 Under a single origin of winter brown camouflage, we would expect the winter-brown AK  
331 individual to nest within the black-tailed jackrabbit clade with the other winter-brown snowshoe

332 hares from the PNW. However, our phylogenetic analysis indicates the winter-brown AK  
333 individual unambiguously groups with a winter-white Boreal individual from PA (100%  
334 bootstrap support), and more broadly with other winter-white hares across the range (Fig. 3).  
335 These results demonstrate that the winter-brown phenotype of this AK hare is caused by  
336 mutations that are independent from the introgressed *Agouti* haplotype that encodes winter-  
337 brown camouflage in the PNW, approximately 3000 km away. Determining the genetic basis of  
338 this independent origin of winter brown camouflage will likely require an independent genetic  
339 association study in these populations.

340 Pooled whole genome sequencing detected that the recessive winter-brown *Agouti* allele  
341 occurs at an estimated frequency of 1.24% ( $\pm 0.01\%$ ) across predominately winter-white MT  
342 localities ~600 km from the polymorphic zone. Interestingly, long-term live-trapping and  
343 radiotelemetry-based field work from this region has resulted in a single observation of a winter-  
344 brown hare in approximately 300 winter hare observations (0.33%; Scott Mills pers. obs.),  
345 although this observed frequency is slightly higher than the Hardy-Weinberg expectation under  
346 the estimated frequency of the winter-brown *Agouti* allele ( $p^2=0.015\%$ , binomial test  $p$ -  
347 value=0.044).

348 To understand the factors that have shaped the geographic distribution of the PNW  
349 *Agouti* allele, we modelled the relative probability of adaptation through independent mutation  
350 with distance from a focal habitat using the theoretical framework of Ralph and Coop (2015).  
351 The change in relative probability of adaptation through independent mutation depended strongly  
352 on both the mutation rate and selection coefficient against the allele in intervening habitats (Fig.  
353 4). Stronger selection coefficients produced a more rapid shift in the convergence probability  
354 with distance relative to weaker selection (Fig. 4). For instance, under a high mutation rate to the

355 winter-brown phenotype ( $\mu=4.54e^{-6}$ ) and strong purifying selection ( $s_m=0.01$ ) the probability of  
356 independent adaptation transitioned sharply from  $P=0.1$  at 78 km to  $P=0.9$  at 140 km from a  
357 focal habitat. Under a low mutation rate to the winter-brown phenotype ( $\mu=4.54e^{-8}$ ) and weak  
358 selection ( $s_m=0.0001$ ), independent adaptation was much less likely at close distances, as  
359 expected, and the probability increased more gradually ( $P=0.1$  at 778 km to  $P=0.9$  at 1400 km).

360

### 361 Migration-selection balance

362 Assuming an environmental shift towards less snow results in strong positive selection ( $s=0.01$ )  
363 on standing variation of the recessive (winter-brown) *Agouti* allele in MT, we used simulations  
364 to estimate that the corresponding probability of fixation would be ~81% (95% confidence  
365 intervals: 72.2-87.5%; Fig. 5A), which is consistent with an analytically-derived probability of  
366 78.1%. For an equivalent dominant mutation starting in mutation-selection balance frequency  
367 (0.015%) the simulated probability of fixation was approximately 77% using simulations (95%  
368 confidence intervals: 67.8-84.2%) or 77.9% using the Kimura (1957) equation. Neither estimate  
369 was significantly different from the fixation probability of a recessive mutation ( $p=0.48$ , two-  
370 tailed test of equality of proportions). However, we observed striking differences in the rates of  
371 increase, conditional on fixation, of dominant and recessive mutations following a sudden  
372 environmental change (Fig. 5B). The mean time to fixation was significantly faster ( $p<2.2e^{-16}$ ,  
373 Student's T-test) for a recessive mutation (9645 generations, SD=3609 generations) compared to  
374 a dominant mutation (19445 generations, SD=7273 generations,  $p<2.2e^{-16}$ ). However, as  
375 expected, we see that initial rates of allele frequency change and phenotypic adaptation are  
376 considerably faster for a positively selected dominant mutation (Fig. 5B). For instance, the mean  
377 time for the selected phenotype determined by the recessive mutation to reach a frequency of

378 75% ( $p=0.866$ ) was 8837 generations (SD=3630 generations), compared to 1007 generations  
379 (SD=116 generations) if determined by the dominant mutation. The striking difference in the rate  
380 at which beneficial dominant versus recessive alleles contribute to adaptation is maintained even  
381 up to the point at which the selected phenotype reaches a frequency of 99%, which takes  
382 approximately 9262 generations (SD=3624 generations) for a recessive mutation and only 2030  
383 generations for dominant mutation (SD=141 generations).

384

## 385 **Discussion**

386 A growing number of studies have found evidence for convergent adaptation within and between  
387 species (Dobler et al., 2012; Giska et al., 2019; Harris et al., 2019; Hoekstra & Nachman, 2003;  
388 Marques et al., 2017; Nelson, Jones, Velotta, Dhawanjewar, & Schweizer, 2019; Rosenblum et  
389 al., 2010; Steiner et al., 2008), although we often lack an understanding of the forces that  
390 determine whether local adaptation occurs through independent *de novo* mutations or migration  
391 of pre-existing alleles from other populations (Ralph & Coop, 2015). Our study provides rare  
392 empirical insights into how gene flow, mutation, allelic dominance, and selection interact to  
393 shape the spatial scale and pace of local adaptation to new or changing environments.

394         Understanding the potential for adaptive variation to spread between populations across  
395 large spatial scales requires basic insights into range-wide patterns of population structure and  
396 gene flow. Winter-brown camouflage in snowshoe hares occurs across only ~5% of the total  
397 range but is broadly-distributed from the western edge of the range along the Pacific coast to the  
398 eastern extent of the range in Pennsylvania (Gigliotti et al., 2017; Mills et al., 2018; Nagorsen,  
399 1983). Previous phylogeographic studies based on limited genetic data suggest that this  
400 distribution spans a deep phylogenetic boundary between Boreal and PNW lineages (~2 Myr

401 divergence; Cheng et al. 2014; Melo-Ferreira et al. 2014) with little evidence for gene flow. With  
402 whole exomes ( $n=95$ ), our phylogenetic analysis also supports a deep split but suggests a  
403 substantially more recent divergence time between Boreal and Rockies/PNW lineages than  
404 previously estimated ( $\sim 97$  kya; Fig. 1B). Our more recent estimates may be attributable to the  
405 increased power of whole exomes or heavy reliance on mitochondrial DNA in previous studies  
406 (Melo-Ferreira et al., 2014), which can lead to overestimation of divergence times (Zheng, Peng,  
407 Kuro-o, & Zeng, 2011). Consistent with previous studies, our ADMIXTURE analyses and range-  
408 wide effective migration surfaces suggest low gene flow between the PNW and Boreal lineages  
409 (Fig. 1C, Fig. 2A). The absence of observable gene flow is perhaps striking given their close  
410 proximity to each other in western North America. Melo-Ferreira et al. (2014) hypothesized that  
411 these lineages may exhibit incipient reproductive isolation. The evolution of reproductive  
412 isolation between these populations is possible, but given our more recent divergence time  
413 estimates we suggest other factors are likely to contribute to the estimated lack of gene flow. For  
414 example, the low effective migration rates ( $Nm$ ; Fig. 2A) could be partially attributable to  
415 reductions in either population densities ( $N$ ) or dispersal capability near the geographic boundary  
416 of Boreal and PNW lineages ( $m$ ; Petkova et al. 2016), although this region appears to be in core  
417 snowshoe hare habitat. More likely, reduced gene flow may reflect quite recent secondary  
418 contact between these populations in western North America. Genetic and fossil evidence  
419 suggests the common ancestors of PNW and Boreal populations occupied separate refugia in  
420 southern and eastern North America, respectively, during the last glacial maximum (Cheng et al.,  
421 2014). The east-to-west phylogenetic clustering (Fig. 1B) and genetic diversity gradient (Fig.  
422 2B) of the Boreal population is consistent with a recent range expansion from this eastern refugia  
423 (Cheng et al. 2014), which implies the PNW and Boreal hares have only recently experienced

424 secondary contact. However, more detailed population history modeling and sampling of the  
425 putative contact zone is required to test these hypotheses.

426 Consistent with low historical gene flow, the AK winter-brown hare lacks the PNW  
427 winter-brown *Agouti* haplotype (Fig. 3), indicating a role for independent mutation leading to the  
428 convergent evolution of brown winter coats. This likely reflects constraints on the migration of  
429 adaptive variation between populations. As previously mentioned, it is unclear if population  
430 structure between Boreal and PNW hares reflects nascent barriers to gene flow (Melo-Ferreira et  
431 al., 2014). Even in the absence of intrinsic or extrinsic reproductive isolation, the rate at which a  
432 positively selected variant spreads across a uniform environment is constrained by dispersal  
433 distance and the strength of positive selection (Fisher 1937). Across spatially or temporally  
434 heterogenous landscapes, the spread of an adaptive allele between patches is further constrained  
435 by the strength or frequency of purifying selection in maladaptive habitats or climatic periods  
436 (Ralph & Coop, 2015). Given that previous models suggest a low probability of winter-brown  
437 camouflage along the majority of the Pacific coast (Mills et al., 2018), we suspect that the  
438 winter-brown PNW variant would have to traverse snowy habitats where it is strongly disfavored  
439 in order to reach Alaska, ~3000 away via the coast. At this distance, the probability of adaptation  
440 through gene flow is virtually zero under a range of model assumptions (Fig. 4). In fact, dispersal  
441 limitations and patchy range-edge habitats should generally favor independent evolution of  
442 winter-brown camouflage at scales beyond 100-1000 km (depending on the assumed values of  $\mu$   
443 and  $s_m$ ; Fig. 4). Further research is needed to dissect the genetic basis of winter-brown  
444 camouflage in the northwestern and eastern edges of the range (e.g., Alaska and Pennsylvania).  
445 Subtle phenotypic similarities between observed winter-brown hares in Alaska and Pennsylvania  
446 could imply a shared genetic basis (e.g., white feet versus brown feet in the PNW, unpublished

447 data). However, our theoretical modelling would suggest that they likely reflect independent  
448 mutations as well (i.e., ~5900 km between AK and PA sampling sites).

449         Convergent evolution is thought to be more common for ‘loss-of-function’ traits because  
450 they may have a larger mutational target size relative to ‘gain-of-function’ traits (Manceau,  
451 Domingues, Mallarino, & Hoekstra, 2011; Rosenblum et al., 2010). Convergent color adaptation  
452 involving loss-of-function mutations has been shown between different species of lizard (Laurent  
453 et al., 2016; Rosenblum et al., 2010) and cavefish (Protas et al., 2006) and the repeated evolution  
454 of melanism across populations of deer mice involves convergent loss-of-function *Agouti*  
455 mutations (Kingsley, Manceau, Wiley, & Hoekstra, 2009). In PNW hares, adaptive introgression  
456 of *Agouti* variation from black-tailed jackrabbits appears to have caused a reversion to the  
457 ancestral winter-brown condition in *Lepus* (i.e., the likely ancestral state before the common  
458 ancestor of winter-white *Lepus* species). As the ancestral winter-brown variant is recessive, this  
459 implies that derived winter-white camouflage in snowshoe hares evolved through dominant gain-  
460 of-function mutations, consistent with the seasonal upregulation of *Agouti* during the  
461 development of white coats (Jones et al., 2018). Independent origins of winter-brown  
462 camouflage across the snowshoe hare range could similarly involve relatively simple loss-of-  
463 function mutations that break the molecular pathways contributing to the development of white  
464 winter coats. Indeed, the evolution of darkened winter coats in some populations of mountain  
465 hares (*Lepus timidus*) appears to have also involved introgression of a recessive, loss-of-function  
466 *Agouti* variant (Giska et al., 2019). Collectively, our results suggest that geographic distance and  
467 mutational target size, in addition to population structure and history, should play a crucial role  
468 in generating hypotheses about the relative roles of independent mutation and gene flow in  
469 adaptation.

470           Despite the evidence for independent winter-brown mutations at broad spatial scales, we  
471 also find that the PNW *Agouti* allele has traversed a substantial distance (~600 km) to western  
472 Montana – a predominately winter-white locality – where it occurs at a frequency of 1.24%. At  
473 this starting frequency, both theory and simulations show that a shift in environmental conditions  
474 towards favoring the brown allele results in a ~80% probability of fixation (Fig. 5). The high  
475 probability of adaptation through gene flow ~600 km from a focal patch is consistent with a  
476 scenario of very weak purifying selection ( $s_m=0.0001$ ) against the winter-brown allele in snowy  
477 environments under the Ralph and Coop (2015) model ( $P(\text{independent mutation})\approx 3\%$   
478 ( $\mu=4.54e-8$ ) or ~76% ( $\mu=4.54e-6$ ); Fig. 4). Although winter-brown camouflage is likely more  
479 strongly deleterious in winter-white environments given the known fitness consequences of  
480 mismatch (Zimova et al., 2016), purifying selection against the winter-brown *Agouti* allele in  
481 winter-white environments may be weak or absent because it is recessive and thus hidden to  
482 selection at low frequency. In agreement with Ralph and Coop (2015), we suggest that  
483 adaptation between distant populations via gene flow may be relatively more common through  
484 recessive variation compared to dominant variation when purifying selection is strong in  
485 intervening habitats.

486           Climate change is expected to reduce winter snow cover across the snowshoe hare range  
487 (Mills et al., 2013), which could potentially result in winter-brown camouflage being favored in  
488 predominately winter-white populations (Mills et al., 2018). Under this scenario, positive  
489 selection could operate on convergent *de novo* winter-brown mutations or on standing genetic  
490 variation for winter-brown camouflage to facilitate rapid adaptation. Using simulations of  
491 positive selection, we show that although dominant and recessive mutations in  
492 mutation/migration-selection balance share a similar fixation probability (Fig. 5A), they are

493 likely to experience vastly different frequency change dynamics (Teshima and Przeworski 2006;  
494 Fig. 5B) and thus lead to very different rates of adaptation following environmental change. For  
495 instance, we show that in MT the initial rate of adaptation from segregating winter-brown *Agouti*  
496 variation is likely to be slow relative to an equivalently beneficial dominant mutation. While  
497 recessive mutations tended to fix more quickly than dominant mutations, they also took  
498 substantially longer to reach high frequencies in populations (Fig. 5B; e.g., 8837 vs. 1007  
499 generations for a phenotype determined by recessive vs. dominant mutation to reach a population  
500 frequency of 75%, respectively). This pattern can be explained by the different allele frequency  
501 phases most strongly affected by genetic drift. For instance, positive selection can readily act on  
502 beneficial dominant mutations at low frequency, but at high frequency the recessive wildtype  
503 allele is hidden in heterozygotes and genetic drift governs (and generally slows) fixation  
504 dynamics. The opposite is true for beneficial recessive mutations, which are governed by genetic  
505 drift at low frequency but driven to fixation by selection. Overall, selection on low frequency  
506 recessive variation may be a relatively ineffective way to adapt rapidly to changing  
507 environments. In fact, the temporal lag for the spread of beneficial recessive variation may be  
508 sufficient enough to allow time for dominant independent mutations (e.g., gain-of-function  
509 MC1R mutations that result in melanism; Nachman et al. 2003b) to appear and spread before the  
510 recessive allele increases appreciably. These findings highlight the important roles of genetic  
511 dominance in shaping both the geographic scope and rate of convergent adaptation and  
512 underscores the need for further study.

513         Collectively, our study provides important insights into long-standing evolutionary  
514 questions, as well as the potential for adaptation to climate change in snowshoe hares. A key to  
515 understanding the potential of adaptive variation to spread under climate change is revealing how

516 it has spread in the past. We show that adaptive responses to reduced snow cover in snowshoe  
517 hares have involved both the local spread of winter-brown camouflage in the PNW as well as  
518 convergent evolution elsewhere in the range. In snowshoe hares and other seasonally changing  
519 species, regions of winter-camouflage polymorphism may be crucial areas to maintain  
520 population connectivity as a conduits for the spread of winter-brown camouflage across broader  
521 portions of the range (Mills et al., 2018). However, facilitating gene flow alone may not be  
522 sufficient to facilitate rapid adaptive responses, given the broad range of snowshoe hares and the  
523 genetic architecture of winter-brown camouflage variation. Rather, we suspect that rapid climate  
524 change responses in winter-white populations distant from winter-brown habitat may also likely  
525 involve independent origins of winter-brown camouflage and selection on variation in coat color  
526 phenology (i.e., shifts in the timing of winter-white molts). Although the genetic basis of  
527 variation in camouflage phenology remains unresolved in this system, it is likely quantitative and  
528 perhaps more responsive to selection. Regardless, this study represents an important step towards  
529 making predictions about evolutionary responses under climate change in this species.

530

### 531 **Data availability**

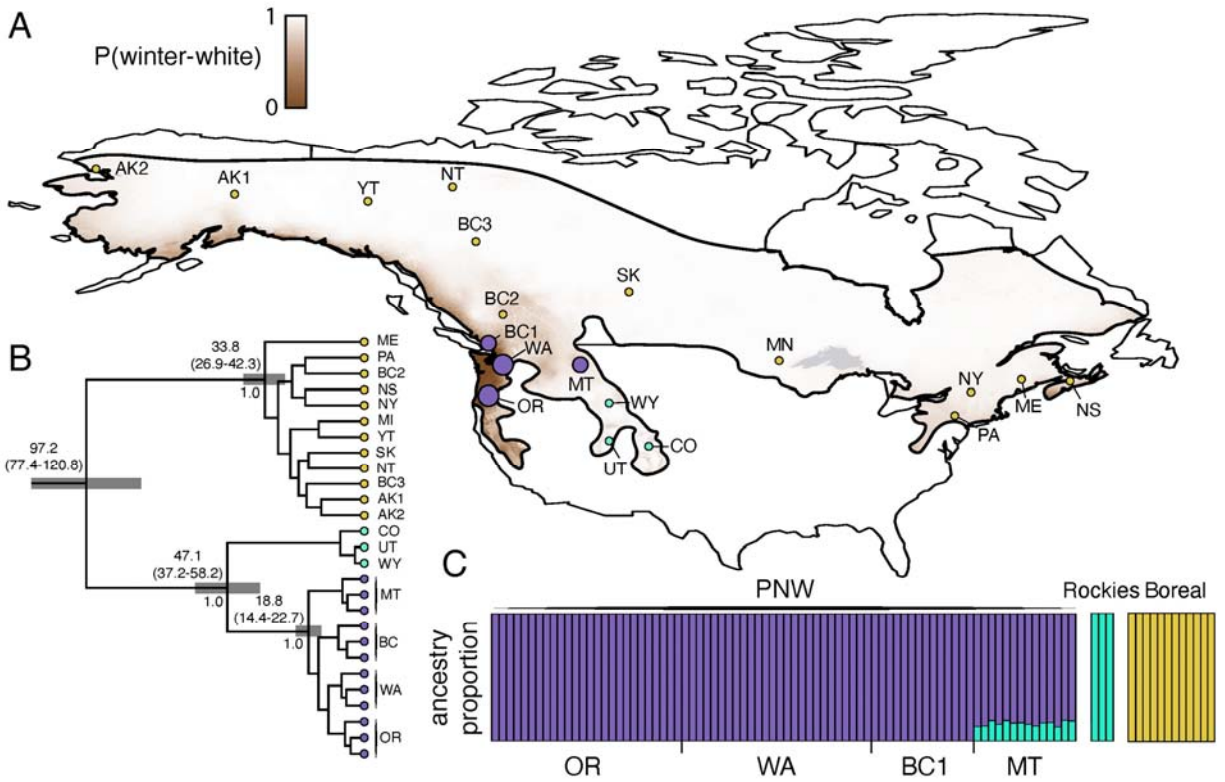
532 Original sequence data are available in the Sequence Read Archive ([www.ncbi.nlm.nih.gov/sra](http://www.ncbi.nlm.nih.gov/sra)).

533 Previously generated whole exome and genome sequence data of snowshoe hare (BioProject  
534 PRJNA420081, SAMN02782769, SAMN07526959) are also available in the Sequence Read  
535 Archive.

536

### 537 **Acknowledgements**

538 We thank E. Cheng and K. Garrison for assistance with sample collection. We thank L. Olson for  
539 informing us on the recent collection of a winter brown snowshoe hare, and L. Olson and the  
540 University of Alaska Museum of the North facilitating a tissue loan of this specimen (UAM  
541 116170). Our research would not be possible without the incredible and irreplaceable support of  
542 natural history museums. We thank J. Melo-Ferreira, P. C. Alves, M. S. Ferreira, N. Herrera, E.  
543 Kopania, A. Kumar, M. Zimova, K. Garrison, and the UNVEIL network for helpful discussions.  
544 Funding and support for this research was provided a National Science Foundation (NSF)  
545 Graduate Research Fellowship (DGE-1313190), NSF Doctoral Dissertation Improvement Grant  
546 (DGE-1702043), NSF Graduate Research Opportunities Worldwide, NSF EPSCoR (OIA-  
547 1736249), and NSF (DEB-0841884; DEB-1907022), the Drollinger-Dial Foundation, American  
548 Society of Mammalogists Grant-in-aid of Research, and a Swiss Government Excellence  
549 Scholarship.



550

551 **Figure 1.** (A) Range-wide phylogeography of snowshoe hares based on whole exome sequences.

552 The snowshoe hare range is colored brown to gray according to the modelled probability of

553 winter-brown camouflage from Mills et al. (2018). Sizes of sampling locality circles are scaled to

554 sample size and are colored according to their population assignment (see C). (B) A maximum

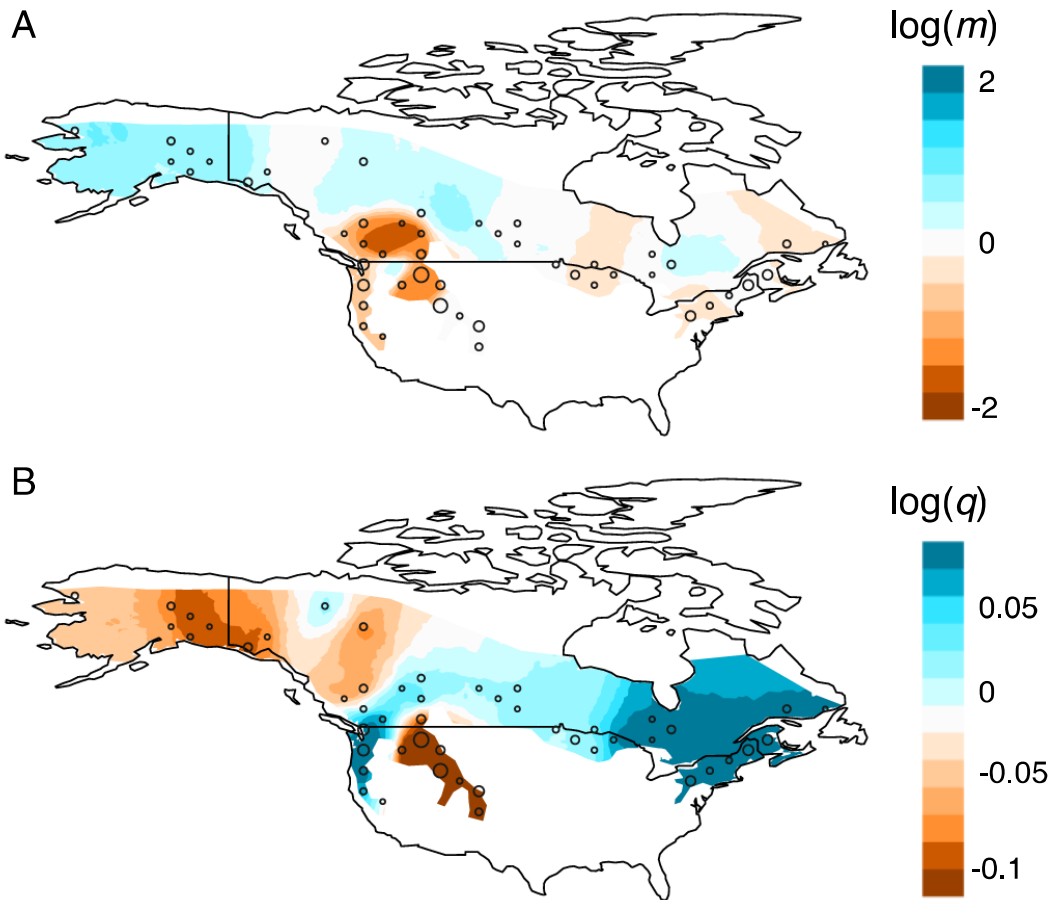
555 credibility phylogenetic tree estimated with BEAST 2 (Bouckaert et al., 2014). All nodes have

556 posterior probabilities >99%. Each major node shows the median node age in thousands of years

557 (95% posterior density in parentheses and gray rectangles) and the ASTRAL support score. (C)

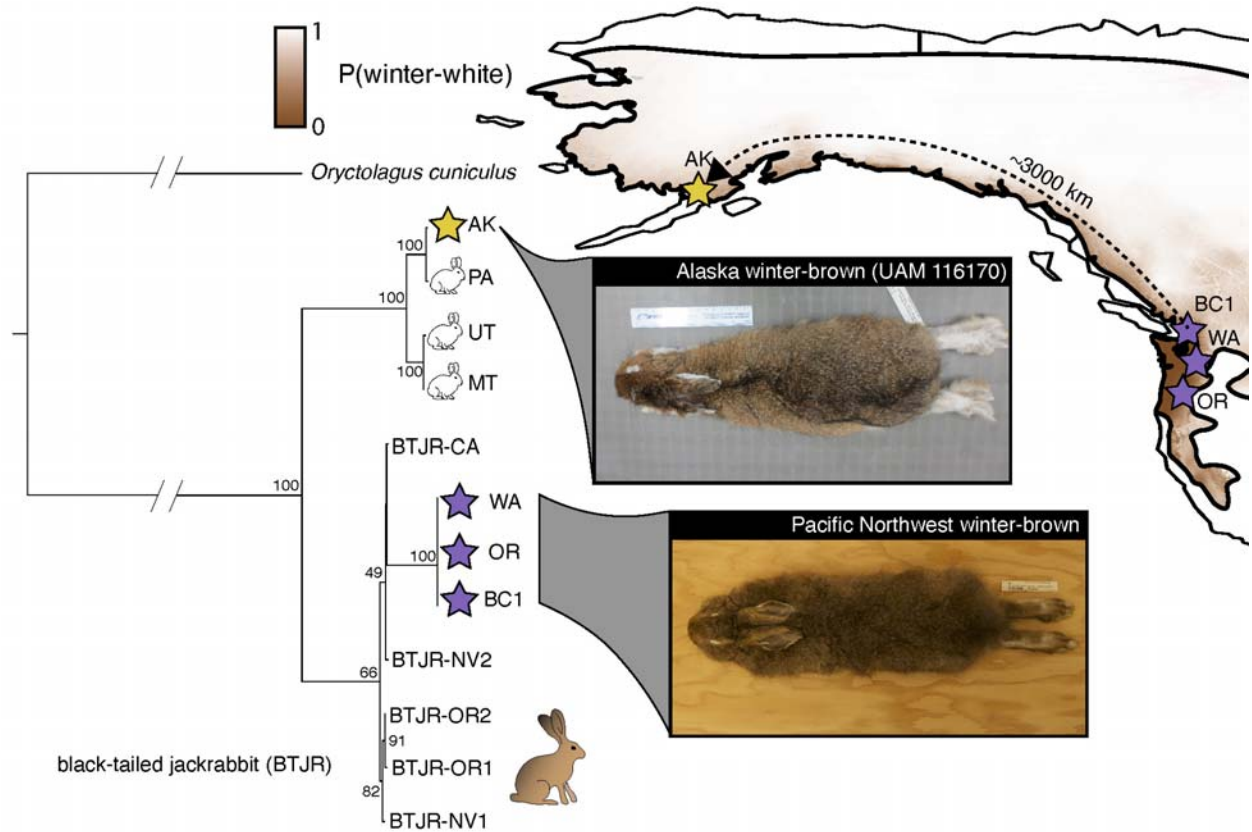
558 The ADMIXTURE plot shows the proportion of ancestry across samples based on a  $K=3$  clustering,

559 which had the lowest cross validation error.



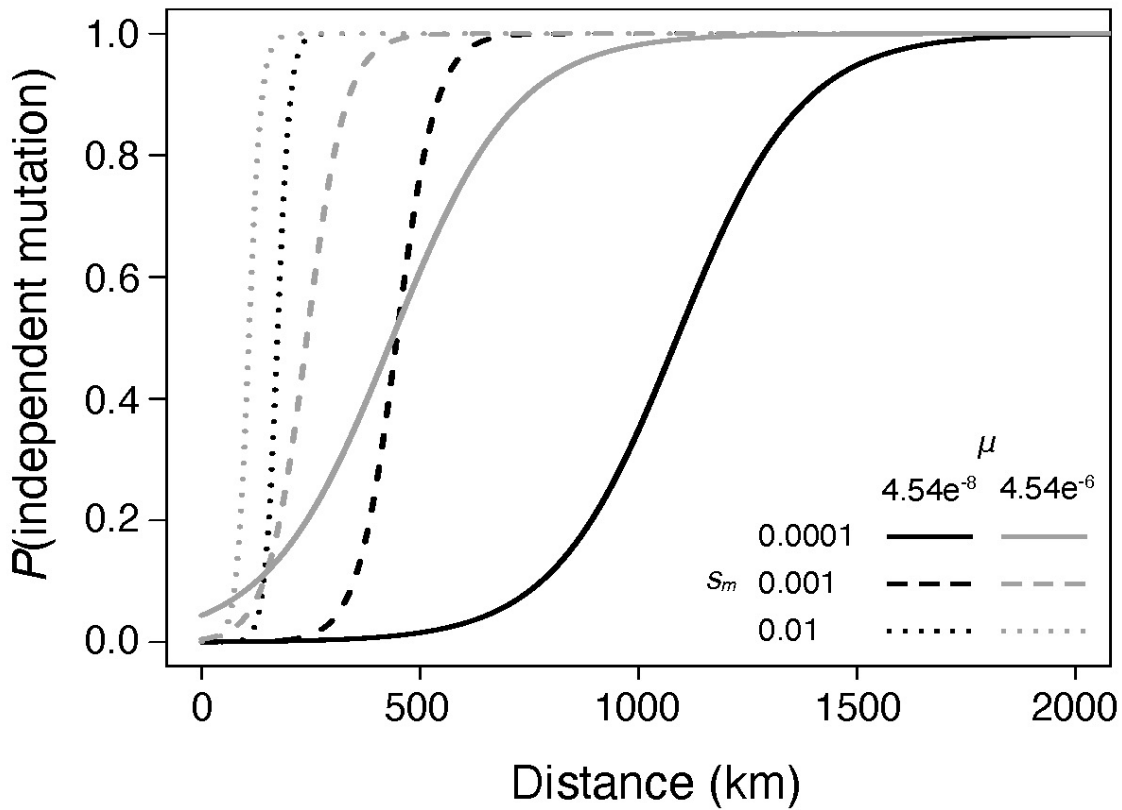
560

561 **Figure 2.** (A) Effective migration rates for snowshoe hares inferred from range-wide  
 562 microsatellite data set (853 individuals, 8 loci) from Cheng et al. (2014). The sizes of circles are  
 563 scaled to the number of samples collected at that location. Effective migration rate is measured  
 564 as the rate of decay in genetic similarity of individuals across space. Regions that are colored  
 565 white are characterized by isolation-by-distance while regions that are colored blue or red have  
 566 higher or lower effective migration, respectively. (B) Effective diversity rates based on the same  
 567 microsatellite data set. Here effective diversity rates measure the genetic dissimilarity between  
 568 individuals in the same deme, where blue regions have higher than average diversity and red  
 569 regions have lower than average diversity.



570

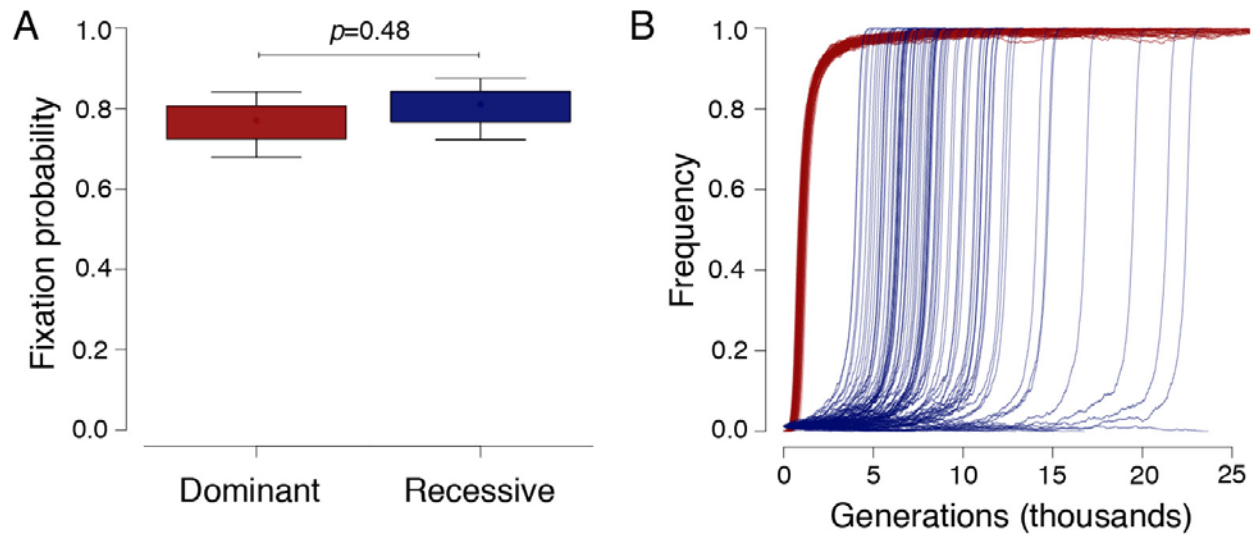
571 **Figure 3.** A maximum clade credibility tree of the introgressed *Agouti* locus (~293 kb) based on  
 572 whole genome sequencing of black-tailed jackrabbits (BTJR; black circles) and snowshoe hares.  
 573 Values indicate node support based on bootstrapping. Colored stars indicate winter-brown  
 574 snowshoe hares from Alaska (yellow, UAM 116170 pictured top) or the Pacific Northwest  
 575 (purple, pictured bottom).



576

577 **Figure 4.** The probability of adaptation through independent mutations in snowshoe hares as a  
 578 function of distance in kilometers from a focal habitat patch harboring a locally adaptive variant.

579 The probability of independent mutation is calculated according to equation 12 in Ralph and  
 580 Coop (2015). Here we varied the mutation rate to the winter-brown phenotype ( $\mu$ ; black= $4.54e^{-8}$ ,  
 581 gray= $4.54e^{-6}$ ) and the negative selection coefficient in intervening habitats ( $s_m$ ; solid line= $0.0001$ ,  
 582 dashed line= $0.001$ , dotted line= $0.01$ ).



583

584 **Figure 5.** (A) The simulated probability of fixation of a completely dominant (red, mean=77%,  
 585  $N=100$ ) or recessive (blue, mean=81%,  $N=100$ ) mutation experiencing positive selection and  
 586 starting in migration-selection balance frequency (0.015% for dominant, 1.24% for recessive).

587 (B) The simulated allele frequency trajectories of the same dominant (blue) and recessive (red)  
 588 mutations starting in migration-selection balance.

589 **Table 1.** Counts of the number of private (e.g., Boreal/Boreal) versus shared SNPs (e.g.,  
 590 Rockies/Boreal) for each major snowshoe hare clade. Individuals from WA represent the PNW.

	Boreal ( <i>N</i> =120978 SNPs)	Rockies ( <i>N</i> =158207 SNPs)	PNW ( <i>N</i> =275614 SNPs)
Boreal	106051	3760	5820
Rockies & PNW	5347	-	-
Rockies	-	117863	31237
PNW	-	-	233210

591

592 **References**

- 593 Alexander, D. H., Novembre, J., & Lange, K. (2009). Fast model-based estimation of ancestry in  
594 unrelated individuals. *Genome Research*, *19*(9), 1655–1664. doi: 10.1101/gr.094052.109
- 595 Barrett, R. D. H., Laurent, S., Mallarino, R., Pfeifer, S. P., Xu, C. C. Y., Foll, M., ... Hoekstra,  
596 H. E. (2019). Linking a mutation to survival in wild mice. *Science*, *363*(6426), 499–504.  
597 doi: 10.1126/science.aav3824
- 598 Bay, R. A., Rose, N., Barrett, R., Bernatchez, L., Ghalambor, C. K., Lasky, J. R., ... Ralph, P.  
599 (2017). Predicting responses to contemporary environmental change using evolutionary  
600 response architectures. *The American Naturalist*, *189*, 463–473. doi: 10.1086/691233
- 601 Bolger, A. M., Lohse, M., & Usadel, B. (2014). Trimmomatic: a flexible trimmer for Illumina  
602 sequence data. *Bioinformatics*, *30*(15), 2114–2120. doi: 10.1093/bioinformatics/btu170
- 603 Bouckaert, R., Heled, J., Kühnert, D., Vaughan, T., Wu, C.-H., Xie, D., ... Drummond, A. J.  
604 (2014). BEAST 2: a software platform for bayesian evolutionary analysis. *PLoS*  
605 *Computational Biology*, *10*(4), e1003537. doi: 10.1371/journal.pcbi.1003537
- 606 Bridle, J. R., & Vines, T. H. (2007). Limits to evolution at range margins: when and why does  
607 adaptation fail? *Trends in Ecology & Evolution*, *22*(3), 140–147. doi:  
608 10.1016/j.tree.2006.11.002
- 609 Brown, R. D., & Mote, P. W. (2009). The response of northern hemisphere snow cover to a  
610 changing climate. *Journal of Climate*, *22*(8), 2124–2145. doi: 10.1175/2008JCLI2665.1
- 611 Carneiro, M., Albert, F. W., Melo-Ferreira, J., Galtier, N., Gayral, P., Blanco-Aguiar, J. A., ...  
612 Ferrand, N. (2012). Evidence for widespread positive and purifying selection across the  
613 European rabbit (*Oryctolagus cuniculus*) genome. *Molecular Biology and Evolution*, *29*(7),  
614 1837–1849. doi: 10.1093/molbev/mss025
- 615 Cheng, E., Hodges, K. E., Melo-Ferreira, J., Alves, P. C., & Mills, L. S. (2014). Conservation  
616 implications of the evolutionary history and genetic diversity hotspots of the snowshoe hare.  
617 *Molecular Ecology*, *23*(12), 2929–2942. doi: 10.1111/mec.12790
- 618 Danecek, P., Auton, A., Abecasis, G., Albers, C. A., Banks, E., DePristo, M. A., ... Durbin, R.  
619 (2011). The variant call format and VCFtools. *Bioinformatics*, *27*(15), 2156–2158. doi:  
620 10.1093/bioinformatics/btr330
- 621 Dobler, S., Dalla, S., Wagschal, V., & Agrawal, A. A. (2012). Community-wide convergent  
622 evolution in insect adaptation to toxic cardenolides by substitutions in the Na,K-ATPase.  
623 *Proceedings of the National Academy of Sciences of the United States of America*, *109*(32),  
624 13040–13045. doi: 10.1073/pnas.1202111109
- 625 Fisher, R. A. (1937). The wave of advance of advantageous genes. *Annals of Eugenics*, *7*(4),  
626 355–369. doi: 10.1111/j.1469-1809.1937.tb02153.x
- 627 Gigliotti, L. C., Diefenbach, D. R., & Sheriff, M. J. (2017). Geographic variation in winter  
628 adaptations of snowshoe hares (*Lepus americanus*). *Canadian Journal of Zoology*, *95*(8),  
629 539–545. doi: 10.1139/cjz-2016-0165
- 630 Gillis, E. A., & Krebs, C. J. (1999). Natal dispersal of snowshoe hares during a cyclic population  
631 increase. *Journal of Mammalogy*, *80*, 933–939. doi: 10.2307/1383263
- 632 Giska, I., Farello, L., Pimenta, J., Seixas, F. A., Ferreira, M. S., Marques, J. P., ... Melo-Ferreira,  
633 J. (2019). Introgession drives repeated evolution of winter coat color polymorphism in  
634 hares. *Proceedings of the National Academy of Sciences of the United States of America*.  
635 doi: 10.1073/pnas.1910471116
- 636 Haldane, J. B. S. (1924). A mathematical theory of natural and artificial selection (Part I).  
637 *Transactions of the Cambridge Philosophical Society*, *23*, 19–41.

638 Haldane, J. B. S. (1932). *The causes of evolution*. London: Longmans, Green and Co.

639 Haller, B. C., & Messer, P. W. (2019). SLiM 3: Forward genetic simulations beyond the Wright-  
640 Fisher model. *Molecular Biology and Evolution*, 36(3), 632–637. doi: 10.1101/418657

641 Harris, R. B., Irwin, K., Jones, M. R., Laurent, S., Barrett, R. D. H., Nachman, R. D. H., ...  
642 Pfeifer, S. P. (2019). The population genetics of crypsis in vertebrates: recent insights from  
643 mice, hares, and lizards. *Heredity*, doi:10.1038/s41437-019-0257-4.

644 Hoekstra, H. E., Drumm, K. E., & Nachman, M. W. (2004). Ecological genetics of adaptive  
645 color polymorphism in pocket mice: Geographic variation in selected and neutral genes.  
646 *Evolution*, 58(6), 1329–1341. doi: 10.1111/j.0014-3820.2004.tb01711.x

647 Hoekstra, H. E., Krenz, J. G., & Nachman, M. W. (2005). Local adaptation in the rock pocket  
648 mouse (*Chaetodipus intermedius*): Natural selection and phylogenetic history of  
649 populations. *Heredity*, 94(2), 217–228. doi: 10.1038/sj.hdy.6800600

650 Hoekstra, H. E., & Nachman, M. W. (2003). Different genes underlie adaptive melanism in  
651 different populations of rock pocket mice. *Molecular Ecology*, 12(5), 1185–1194. doi:  
652 10.1046/j.1365-294X.2003.01788.x

653 Hoffmann, A. A., & Sgrò, C. M. (2011). Climate change and evolutionary adaptation. *Nature*,  
654 470(7335), 479–485. doi: 10.1038/nature09670

655 Jones, M. R., Mills, L. S., Alves, P. C., Callahan, C. M., Alves, J. M., Lafferty, D. J. R., ...  
656 Good, J. M. (2018). Adaptive introgression underlies polymorphic seasonal camouflage in  
657 snowshoe hares. *Science*, 360(6395), 1355–1358. doi: 10.1126/science.aar5273

658 Kimura, M. (1957). Some Problems of Stochastic Processes in Genetics. *The Annals of*  
659 *Mathematical Statistics*, 28(4), 882–901. doi: 10.1214/aoms/1177706791

660 Kingsley, E. P., Manceau, M., Wiley, C. D., & Hoekstra, H. E. (2009). Melanism in *Peromyscus*  
661 is caused by independent mutations in *Agouti*. *PLoS ONE*, 4(7), e6435. doi:  
662 10.1371/journal.pone.0006435

663 Knowles, N., Dettinger, M. D., Cayan, D. R., Knowles, N., Dettinger, M. D., & Cayan, D. R.  
664 (2006). Trends in snowfall versus rainfall in the western United States. *Journal of Climate*,  
665 19(18), 4545–4559. doi: 10.1175/JCLI3850.1

666 Kofler, R., Orozco-terWengel, P., De Maio, N., Pandey, R. V., Nolte, V., Futschik, A., ...  
667 Schlötterer, C. (2011). PoPoolation: a toolbox for population genetic analysis of next  
668 generation sequencing data from pooled individuals. *PLoS ONE*, 6(1), e15925. doi:  
669 10.1371/journal.pone.0015925

670 Kreiner, J. M., Giacomini, D. A., Bemm, F., Waithaka, B., Regalado, J., Lanz, C., ... Wright, S.  
671 I. (2019). Multiple modes of convergent adaptation in the spread of glyphosate-resistant  
672 *Amaranthus tuberculatus*. *Proceedings of the National Academy of Sciences*, 201900870.  
673 doi: 10.1073/pnas.1900870116

674 Laurent, S., Pfeifer, S. P., Settles, M. L., Hunter, S. S., Hardwick, K. M., Ormond, L., ...  
675 Rosenblum, E. B. (2016). The population genomics of rapid adaptation: disentangling  
676 signatures of selection and demography in white sands lizards. *Molecular Ecology*, 25(1),  
677 306–323. doi: 10.1111/mec.13385

678 Li, H. (2013). Aligning sequence reads, clone sequences and assembly contigs with BWA-MEM.  
679 *ArXiv*, 1303.3997. Retrieved from <http://arxiv.org/abs/1303.3997>

680 Magoč, T., & Salzberg, S. L. (2011). FLASH: fast length adjustment of short reads to improve  
681 genome assemblies. *Bioinformatics*, 27(21), 2957–2963. doi: 10.1093/bioinformatics/btr507

682 Manceau, M., Domingues, V. S., Mallarino, R., & Hoekstra, H. E. (2011). The developmental  
683 role of *Agouti* in color pattern evolution. *Science*, 331(6020), 1062–1065. doi:

684 10.1126/science.1200684  
685 Marques, D. A., Taylor, J. S., Jones, F. C., Di Palma, F., Kingsley, D. M., & Reimchen, T. E.  
686 (2017). Convergent evolution of SWS2 opsin facilitates adaptive radiation of threespine  
687 stickleback into different light environments. *PLOS Biology*, *15*(4), e2001627. doi:  
688 10.1371/journal.pbio.2001627  
689 McKenna, A., Hanna, M., Banks, E., Sivachenko, A., Cibulskis, K., Kernytsky, A., ... DePristo,  
690 M. A. (2010). The Genome Analysis Toolkit: A MapReduce framework for analyzing next-  
691 generation DNA sequencing data. *Genome Research*, *20*(9), 1297–1303. doi:  
692 10.1101/gr.107524.110  
693 Melo-Ferreira, J., Seixas, F. A., Cheng, E., Mills, L. S., & Alves, P. C. (2014). The hidden  
694 history of the snowshoe hare, *Lepus americanus*: extensive mitochondrial DNA  
695 introgression inferred from multilocus genetic variation. *Molecular Ecology*, *23*(18), 4617–  
696 4630. doi: 10.1111/mec.12886  
697 Milholland, B., Dong, X., Zhang, L., Hao, X., Suh, Y., & Vijg, J. (2017). Differences between  
698 germline and somatic mutation rates in humans and mice. *Nature Communications*, *8*,  
699 15183. doi: 10.1038/ncomms15183  
700 Mills, L. S., Bragina, E. V., Kumar, A. V., Zimova, M., Lafferty, D. J. R., Feltner, J., ... Fay, K.  
701 (2018). Winter color polymorphisms identify global hot spots for evolutionary rescue from  
702 climate change. *Science*, *359*(6379), 1033–1036. doi: 10.1126/science.aan8097  
703 Mills, L. S., Zimova, M., Oyler, J., Running, S., Abatzoglou, J. T., & Lukacs, P. M. (2013).  
704 Camouflage mismatch in seasonal coat color due to decreased snow duration. *Proceedings*  
705 *of the National Academy of Sciences of the United States of America*, *110*(18), 7360–7365.  
706 doi: 10.1073/pnas.1222724110  
707 Nachman, M. W., Hoekstra, H. E., & D'Agostino, S. L. (2003a). The genetic basis of adaptive  
708 melanism in pocket mice. *Proceedings of the National Academy of Sciences of the United*  
709 *States of America*, *100*(9), 5268–5273. doi: 10.1073/pnas.0431157100  
710 Nachman, M. W., Hoekstra, H. E., & D'Agostino, S. L. (2003b). The genetic basis of adaptive  
711 melanism in pocket mice. *Proceedings of the National Academy of Sciences of the United*  
712 *States of America*, *100*(9), 5268–5273. doi: 10.1073/pnas.0431157100  
713 Nagorsen, D. W. (1983). Winter pelage colour in snowshoe hares (*Lepus americanus*) from the  
714 Pacific Northwest. *Canadian Journal of Zoology*, *61*(10), 2313–2318. doi: 10.1139/z83-305  
715 Nelson, T. C., Jones, M. R., Velotta, J. P., Dhawanjewar, A. S., & Schweizer, R. M. (2019).  
716 UNVEILing connections between genotype, phenotype, and fitness in natural populations.  
717 *Molecular Ecology*, *28*(8), 1866–1876. doi: 10.1111/mec.15067  
718 Orr, H. A., & Betancourt, A. J. (2001). Haldane's sieve and adaptation from the standing genetic  
719 variation. *Genetics*, *157*(2), 875–884.  
720 Petkova, D., Novembre, J., & Stephens, M. (2016). Visualizing spatial population structure with  
721 estimated effective migration surfaces. *Nature Genetics*, *48*(1), 94–100. doi:  
722 10.1038/ng.3464  
723 Pfeifer, S. P., Laurent, S., Sousa, V. C., Linnen, C. R., Foll, M., Excoffier, L., ... Jensen, J. D.  
724 (2018). The evolutionary history of Nebraska deer mice: local adaptation in the face of  
725 strong gene flow. *Molecular Biology and Evolution*, *35*, 792–806. doi:  
726 10.1093/molbev/msy004  
727 Protas, M. E., Hersey, C., Kochanek, D., Zhou, Y., Wilkens, H., Jeffery, W. R., ... Tabin, C. J.  
728 (2006). Genetic analysis of cavefish reveals molecular convergence in the evolution of  
729 albinism. *Nature Genetics*, *38*(1), 107–111. doi: 10.1038/ng1700

730 R Core Team. (2018). *R: A language and environment for statistical computing*. Retrieved from  
731 <https://www.r-project.org/>

732 Ralph, P. L., & Coop, G. (2010). Parallel adaptation: One or many waves of advance of an  
733 advantageous allele? *Genetics*, *186*(2), 647–668. doi: 10.1534/genetics.110.119594

734 Ralph, P. L., & Coop, G. (2015). Convergent evolution during local adaptation to patchy  
735 landscapes. *PLOS Genetics*, *11*(11), e1005630. doi: 10.1371/journal.pgen.1005630

736 Rohland, N., & Reich, D. (2012). Cost-effective, high-throughput DNA sequencing libraries for  
737 multiplexed target capture. *Genome Research*, *22*(5), 939–946. doi: 10.1101/gr.128124.111

738 Rosenblum, E. B., Römler, H., Schöneberg, T., & Hoekstra, H. E. (2010). Molecular and  
739 functional basis of phenotypic convergence in white lizards at White Sands. *Proceedings of  
740 the National Academy of Sciences of the United States of America*, *107*(5), 2113–2117. doi:  
741 10.1073/pnas.0911042107

742 Schlager, G., & Dickie, M. M. (1971). Natural mutation rates in the house mouse. Estimates for  
743 five specific loci and dominant mutations. *Mutation Research*, *11*(1), 89–96. doi:  
744 10.1016/0027-5107(71)90034-0

745 Slatkin, M. (1973). Gene flow and selection in a cline. *Genetics*, *75*(4), 733–756. Retrieved from  
746 <http://www.ncbi.nlm.nih.gov/pubmed/4778791>

747 Stamatakis, A. (2014). RAxML version 8: a tool for phylogenetic analysis and post-analysis of  
748 large phylogenies. *Bioinformatics*, *30*(9), 1312–1313. doi: 10.1093/bioinformatics/btu033

749 Steiner, C. C., Rompler, H., Boettger, L. M., Schoneberg, T., & Hoekstra, H. E. (2008). The  
750 genetic basis of phenotypic convergence in beach mice: similar pigment patterns but  
751 different genes. *Molecular Biology and Evolution*, *26*(1), 35–45. doi:  
752 10.1093/molbev/msn218

753 Teshima, K. M., & Przeworski, M. (2006). Directional positive selection on an allele of arbitrary  
754 dominance. *Genetics*, *172*(1), 713–718. doi: 10.1534/genetics.105.044065

755 Turner, J. R. G. (1981). Adaptation and evolution in *Heliconius*: a defense of NeoDarwinism.  
756 *Annual Review of Ecology and Systematics*, *12*, 99–121. doi:  
757 10.1146/annurev.es.12.110181.000531

758 Wright, S. (1931). Evolution in Mendelian populations. *Genetics*, *16*, 97–159.

759 Zhang, C., Rabiee, M., Sayyari, E., & Mirarab, S. (2018). ASTRAL-III: Polynomial time species  
760 tree reconstruction from partially resolved gene trees. *BMC Bioinformatics*, *19*. doi:  
761 10.1186/s12859-018-2129-y

762 Zheng, Y., Peng, R., Kuro-o, M., & Zeng, X. (2011). Exploring patterns and extent of bias in  
763 estimating divergence time from mitochondrial DNA sequence data in a particular lineage:  
764 a case study of salamanders (Order Caudata). *Molecular Biology and Evolution*, *28*(9),  
765 2521–2535. doi: 10.1093/molbev/msr072

766 Zimova, M., Hackländer, K., Good, J. M., Melo-Ferreira, J., Alves, P. C., & Mills, L. S. (2018).  
767 Function and underlying mechanisms of seasonal colour moulting in mammals and birds:  
768 what keeps them changing in a warming world? *Biological Reviews*, *93*(3), 1478–1498. doi:  
769 10.1111/brv.12405

770 Zimova, M., Mills, L. S., & Nowak, J. J. (2016). High fitness costs of climate change-induced  
771 camouflage mismatch. *Ecology Letters*, *19*(3), 299–307. doi: 10.1111/ele.12568

772